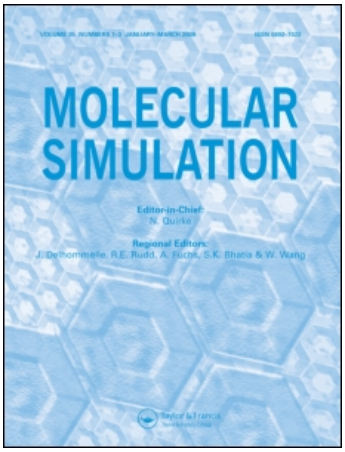

Molecular Simulation
Publication details, including instructions for authors and subscription information:
http://www.informaworld.com/smpp/title~content=t713644482

Monte Carlo Simulation Study of Adsorption Characteristics in Slit-Like Micropores Under Supercritical Conditions

T. Shigeta[a]; J. Yoneya[a]; T. Nitta[a]
[a] Dept. of Chemical Engineering, Osaka University, Toyonaka, Osaka, Japan

To cite this Article Shigeta, T. , Yoneya, J. and Nitta, T.(1996) 'Monte Carlo Simulation Study of Adsorption Characteristics in Slit-Like Micropores Under Supercritical Conditions', Molecular Simulation, 16: 4, 291 — 305
To link to this Article: DOI: 10.1080/08927029608024081
URL: http://dx.doi.org/10.1080/08927029608024081

Molecular Simulation, 1996, Vol. 16, pp. 291–305
Reprints available directly from the publisher
Photocopying permitted by license only

MONTE CARLO SIMULATION STUDY OF ADSORPTION CHARACTERISTICS IN SLIT-LIKE MICROPORES UNDER SUPERCRITICAL CONDITIONS

T. SHIGETA, J. YONEYA and T. NITTA*

Dept. of Chemical Engineering, Osaka University, Toyonaka, Osaka 560, Japan

(Received February, 1995, accepted June 1995)

Adsorption characteristics of a solute diluted in supercritical fluids has been investigated by using the Monte Carlo simulation techniques. The Lennard-Jones potential function is used for describing interactions for a model system of CO_2 + benzene in slit-like micropores with infinite graphitic carbon walls. A modified μVT ensemble method with particle exchange proposed by Cracknell, Nicholson and Quirke (1993) is found to be much superior to the conventional μVT ensemble method especially for dense mixtures in a pore. Adsorption isotherms of CO_2 and benzene, in equilibrium with a dilute benzene mixture in CO_2 (mole fraction of benzene = 0.001), are computed by varying pressure, temperature, the benzene–surface interaction potential, and the slitwidth. Adsorption isotherm curve of CO_2 increases with an increase in pressure while that of benzene shows a maximum at a pressure far below the critical pressure of CO_2 and then it decreases with increasing pressure. The decrease in benzene adsorption with increasing pressure is attributable to both the enhanced solubility in supercritical CO_2 and the competitive adsorption of CO_2. The isotherm curves of each component at two temperatures, 313.2 K and 323.2 K, show to cross at a pressure near the critical pressure due to the "density effect" on the chemical potentials of a solute at supercritical fluid conditions. When the interaction between a solute and a surface increases, the adsorption isotherm increases. Narrowing the slitwidth results in the increase in the adsorption of solute since the external potential from two walls becomes deeper.

KEY WORDS: Monte Carlo, grand canonical ensemble, adsorption equilibrium, supercritical fluid, Lennard-Jones potential, binary mixture.

1 INTRODUCTION

Supercritical fluids (SCF) are new type of solvents since their solvent power varies dramatically by changing pressure as well as temperature. Both SCF extraction and SCF chromatography have become new separation techniques calling our attention [1–4]. Recently, combination of adsorption phenomenon with SCF has been used to develop advanced separation processes, such as SCF dewaxing of ceramic green bodies [5], SCF regeneration of activated carbons [6], and adsorptive purification of naphthalene derivatives combined with SCF extraction [7]. In other processes, such as extraction from porous materials or drying powders, adsorption phenomena occur naturally. Understanding the phenomena of adsorption from supercritical fluids has become important.

Computer simulation techniques have been used to analyze the adsorption of gases at SCF conditions [8–11]. However, most of them are designed for single component adsorption, in particular for methane storage technology. Studies on mixed-gas adsorptions in slitlike pores, which are closely related to the adsorption from SCF on commercial activated carbons, are still limited. Sokolowski and Fischer [12] calculated Ar-Kr mixtures in slitpores using the molecular dynamics technique to investigate the applicability of density functional theory (DFT) of Meister, Kroll and Groot [13, 14]. Cracknell, Nicholson and Quirke [15] reported adsorption isotherms of methane-ethane mixtures in slitpores using a new version of the grand canonical ensemble Monte Carlo (GCMC) method; they found that the ideal adsorbed solution theory (IAST) could represent their simulation results better than the DFT given by Tan and Gubbins [16]. A comparison of the mean field DFT with GCMC simulation results for methane–Ar mixtures on a graphite surface was also made by Kierlik *et al.* [17].

We performed computer simulations of mixed-gas adsorptions in slitlike pores at SCF conditions by using the spherical Lennard-Jones potential for representing intermolecular interactions; the fluid systems were binary mixtures of butane and CO_2 [18] and dilute mixture of benzene in CO_2 [19]. The calculation results suggested that the major factors characterizing adsorptions from SCF are the enhanced solubility in the SCF and the competitive adsorption of SCF molecules. The present work is an extension of the latter work [19] to explore the influence of temperature, the slitwidth, and the solute–surface interactions on the adsorption from SCF.

In the first section we briefly describe the model and the simulation methods: the *NVT* ensemble with Widom's test particle insertion method, the conventional and the modified GCMC methods, and the Gibbs ensemble method used for vapor–liquid equilibrium (VLE) calculations. Next we present VLE results for CO_2 + benzene mixtures and a comparison of performance of the two GCMC methods for dense mixtures in a slitpore. Then simulation results are given for binary adsorption isotherms at different temperatures, with different slitwidth or different solute–surface interactions. Finally some concluding remarks will be given.

2 MODEL AND PARAMETERS

We used the Lennard-Jones potential function for describing intermolecular interactions between component 1 (CO_2), component 2 (benzene) and component *s* (graphitic carbon). The pair potential between gas molecules *i* and *j* separated by distance r, $\phi_{ij}(r)$, is described as equation (1).

$$\phi_{ij}(r) = 4\varepsilon_{ij}\left[\left(\frac{\sigma_{ij}}{r}\right)^{12} - \left(\frac{\sigma_{ij}}{r}\right)^{6}\right] \tag{1}$$

We used the potential function between a molecule and a solid surface by '10-4-3' potential, which is denoted as $\phi_{is}(Z)$, where Z is the normal distance between a

molecule and a surface passing through the atomic centers of a basal plane.

$$\phi_{is}(Z) = 4\pi A_{is}\left[\frac{2}{5}\left(\frac{\sigma_{is}}{Z}\right)^{10} - \left(\frac{\sigma_{is}}{Z}\right)^{4} - \frac{\sigma_{is}^{4}}{3\Delta(Z+0.61\Delta)^{3}}\right] \tag{2}$$

where A_{is} ($=\varepsilon_{is}\sigma_{is}^{2}/a_s$) is a constant, a_s the surface area of graphite basal unit, and Δ the spacing between adjacent graphite basal plane. The potential energy Φ_i (Z) for molecule i located at distance Z from a wall surface is calculated as

$$\Phi_i(Z) = \sum_j \phi_{ij}(r_{ij}) + \phi_{is}(Z) + \phi_{is}(H-Z) \tag{3}$$

where H is the slit width and the suffix j runs over different molecules in the pore. The pair potential in a fluid phase is cut off at a distance of min[$3.5\sigma_{22}$, $L_x/2$], where L_x is the length of a simulation box. The long range correction is applied to the fluid region, but not to the pore region where the cut-off radius is essentially $3.5\sigma_{22}$.

The LJ parameters, ε/k and σ, have been determined from the critical constants, T_c and p_c, by adopting the correlation of Nicolas *et al.* [20]: $kT_c/\varepsilon = 1.35$ and $p_c\sigma^3/\varepsilon = 0.142$. However, the potential depth of benzene ε was relaxed to fit the vapor pressure. The LJ parameters used in this work are summarized in Table 1, where the parameters for graphitic carbon atom are taken from those used in the previous work [18, 19], originally suggested by Steele [21]. Different values for ε for benzene are given in the table at two temperatures. We used the Lorentz-Berthelot rule for the cross parameters; that is the arithmetic mean for σ and the geometric mean for ε. We also defined the binary parameter k_{ij} in equation (4).

$$\varepsilon_{ij} = (\varepsilon_{ij}\varepsilon_{ij})^{1/2}(1-k_{ij}) \tag{4}$$

The value of k_{12} is determined from a fit to the vapor-liquid equilibria of CO_2 and benzene binary mixtures [22]; k_{1s} is determined to fir the adsorption isotherms of CO_2 on activated carbon (mesophase carbon M-30) we previously measured [23]. The value of k_{2s} is varied as 0.0, 0.15, and -0.15 to explore the effect of adsorption energy of an adsorbate.

Table 1 LJ parameters used for simulations.

	σ_i [*nm*]	ε_{ii}/k [*K*]
CO_2(1)	0.3910	225.3
C_6H_6(2)	0.5506	468.5(313.2 K) 465.4(323.2 K)
Carbon	0.3400	28.0

$k_{12}=0.1232$, $k_{1s}=0.170$, $k_{2s}=-0.15, 0.0, 0.15$

3 SIMULATION METHODS

The strategy of calculating adsorption equilibrium in contact with a dilute benzene mixture of supercritical CO_2 is as follows: (i) to carry out the NVT ensemble MC computation for pure CO_2 at a specified temperature (T) and density (ρ) with insertions of ghost molecules of CO_2 (component 1) and benzene (component 2) for calculating the residual chemical potentials of each component (μ_1^r, μ_2^r), (ii) to calculate the chemical potentials (μ_1, μ_2) by specifying the mole fractions in a fluid ($y_2 = 0.001$, $y_1 = 1 - y_2$), (iii) to calculate the density (ρ_p) and the mole fractions in a slitpore (x_1, x_2) by performing a GCMC simulation at a specified set of μ_1, μ_2, V_p and T.

We calculate the VLE for a fluid mixture, CO_2 + benzene, at a specified temperature and pressure by use of the Gibbs ensemble MC method [25], which yields the mole fractions of vapor phase (y_i) and liquid phase (x_i) in equilibrium.

3.1 *NVT Ensemble MC Method with Widom's Test Particle Insertion Method*

The chemical potentials of each component, μ_1 and μ_2, have been determined for a binary fluid mixture of the mole fraction $y_2 = 0.001$ by using equation (8)

$$\mu_i = kT \ln \rho^* y_i + \mu_i^r \quad (i = 1, 2) \tag{5}$$

where ρ^* ($= \sigma_{11}^3 \rho$) is the dimensionless density. μ_i^r is calculated by Widom's test particle insertion method, equation (9) [25], which has been embedded in the NVT ensemble MC method.

$$\mu_i^r = -kT \ln \langle \exp(-\beta \Phi_i) \rangle \tag{6}$$

where the symbol $< \cdots >$ denotes the ensemble average. We have used 256 particles of pure CO_2 for calculating μ_i^r of each component since the pure fluid ($y_2 = 0.0$) is practically close enough to yielding the residual chemical potentials in a dilute mixture of $y_2 = 0.001$.

3.2 *Conventional μVT Ensemble Method*

The μVT ensemble MC method has been used for simulating adsorption phenomena by specifying the chemical potential of each component (μ_i), the volume (V) and the temperature (T). This method consists of three steps: (i) displacement movement, (ii) creation of a molecule at a random location, (iii) destruction of a molecule chosen randomly. The transitional probabilities for steps of creation and destruction of molecule of component i are given as

$$P_{\text{create}} = \min \left\{ 1, \frac{z_i V^*}{N_i + 1} \exp(-\beta \Phi_i) \right\} \tag{7}$$

$$P_{\text{destr}} = \min\left\{1, \frac{N_i}{z_i V^*} \exp(\beta \Phi_i)\right\} \tag{8}$$

where N_i is the number of molecules, $\beta = 1/kT$, $z_i = \exp(\beta\mu_i)/\Lambda_i^3$ the absolute activity, $V^* = V/\sigma_{11}^3$, and Λ_i the thermal de Broglie wavelength.

3.3 *μVT Ensemble Method with Particle Exchange*

Numerous different configurations of a system are required to obtain good statistics and accuracy in the MC simulation. The disadvantage of the conventional μVT ensemble is that it is difficult to meet successful trial for the creation and destruction of larger molecule for mixtures of high density. To overcome this problem, Cracknell, Nicholson and Quirke [15] proposed an algorithm for creation and destruction steps of a larger molecule by changing the identity of a particle. Figure 1 is a schematic diagram of the μVT ensemble with particle exchange. Box A shows a displacement step. If we choose a CO_2 molecule (smaller molecule) in an creation or destruction step, a conventional creation or destruction procedure, (B−1) or (B−2), is carried out. However, if we choose a benzene molecule (larger molecule) to be inserted, we pick up a CO_2 molecule randomly and exchange the molecular identity; that is, CO_2 to benzene. Destruction of a benzene molecule is tried by choosing a benzene molecule randomly and exchanging the identity of the benzene molecule to CO_2. Cracknell *et al.* used this version of the μVT ensemble for simulating the mixed adsorption of methane and ethane in a slitpore. When considering a case in which a molecule of component j is exchanged to component i, the probability of the

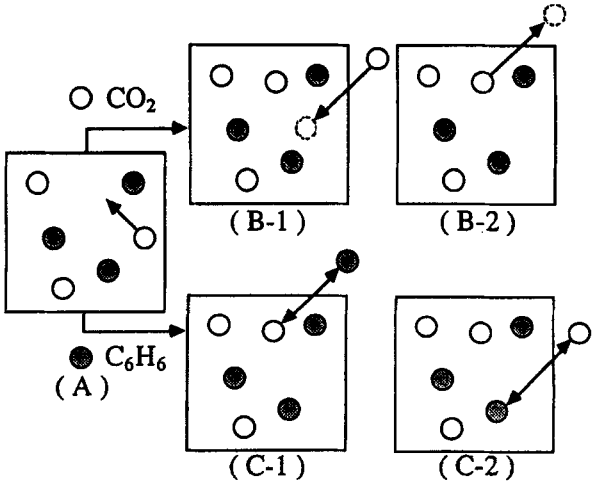

Figure 1 Schematic diagrams of μVT ensemble with particle exchange: (A) displacement, (B) particle creation/destruction: (B-1) CO_2 in, (B-2) CO_2 out, (C) particle exchange: (C-1) benzene in and CO_2 out, (C-2) benzene out and CO_2 in.

exchange is given by

$$P_{\text{exch}} = \min\left[\left\{1, \frac{N_j z_i}{(N_i+1)z_j}\exp\{-\beta(\Phi_i - \Phi_j)\}\right\}\right] \tag{7}$$

In order to maintain microscopic reversibility, the trial numbers of exchanging a molecule of CO_2 to benzene and benzene to CO_2 are kept the same. We used both the conventional μVT and the modified μVT with particle exchange to simulate mixed-gas adsorption at supercritical conditions. In both methods, the box volume V was adjusted to contain about 200–300 total molecules during a simulation. The frequencies of creation and destruction of molecules are set on equal probability for each component; however, the probability of selecting CO_2 and benzene molecules is adjusted so as to obtain almost the same number of acceptance for the two components during a simulation. In the μVT simulation, one cycle consists of 300 displacements. The number of trials for particle transfer per displacement step is within 1 and 10 for the modified μVT ensemble method, and 5 to 150 for the conventional μVT ensemble method. The first 3000 cycles were discarded and the last 5000 cycles were used for ensemble averages.

3.4 *Gibbs Ensemble Method*

The Gibbs ensemble MC method proposed by Panagiotopoulos [24] is designed for directly calculating the concentrations of two phases in equilibrium, such as vapor-liquid (VLE), liquid-liquid, and gas-solid equilibria. The Gibbs ensemble method for VLE uses two regions, region I for a vapor phase and region II for a liquid phase. The simulation comprises three distinct moves: (a) a particle displacement (NVT), (b) a particle transfer (μVT), and (c) a volume rearrangement (NpT). The total number of particles N ($= N^{\text{I}} + N^{\text{II}}$) is preserved during each simulation. In the initial configurations, we set molecules as $N^{\text{I}} = 256$ $N^{\text{II}} = 256$. One cycle consists of 512 displacements in the Gibbs ensemble simulation. The number of trials for particle transfer per displacement trial is set within 1 and 30. The total number of cycles in a simulation is 7500; the first 2500 cycles are discarded and the rest are used for the ensemble averages of mechanical properties in both phases.

4 RESULTS AND DISCUSSION

4.1 *Vapor-Liquid Equilibrium*

Figure 2 shows the pressure-composition diagram for $CO_2(1)+$ benzene (2) mixtures at 313.2 K, the equilibrium data points of which are obtained by the Gibbs ensemble method. The ordinate is the pressure and the abscissa is the mole fraction of CO_2 in vapor phase (y_1) or liquid phase (x_1). When we adjust the binary parameter k_{12} to 0.1232, the agreement between the experimental data of Gupta *et al.* [22] and the simulation points is satisfactory. In addition, this simulation results indicate that a mixture of dilute benzene ($y_2 = 0.001$) keeps homogeneous phases (a gas phase to a supercritical fluid phase) up to high pressures.

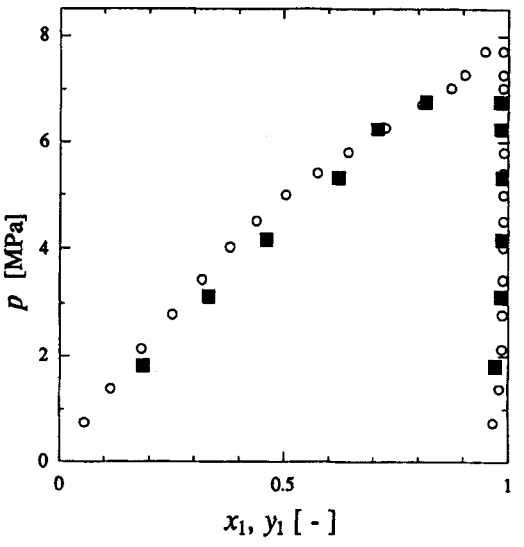

Figure 2 Pressure-composition diagram for $CO_2(1)$ + benzene (2) at 313.2 K: (■); simulation, (○); experimental [Gupta *et al.* 22].

4.2 *Performance of the μVT Ensemble Methods*

Table 2 shows comparisons of performance between the conventional μVT method (1) and the modified μVT method with particle exchange (2). The calculation conditions are $T = 313.2$ K, slitwidth of a pore $H = 1.2$ nm and binary parameter $k_{2s} = 0.0$. All thermodynamic properties in the table are given in reduced units: the density $\rho^* = \rho\sigma_{11}^3$, mole fraction x_i, the internal energy $U^* = U/\varepsilon_{11}$, and the pressure $p^* = p\sigma_{11}^3/\varepsilon_{11}$. Only the pressure was calculated from the NVT ensemble simulations.

The distinguishable difference between the two μVT methods is the frequency of success trials for insertion or destruction of benzene molecules, f_{success}. In the conventional μVT ensemble, the success probability in trials is in the order of 10^{-5} while that is in the order of 10^{-2} to 10^{-3} in the modified μVT ensemble, which is over hundred times larger than the conventional method. This is very important to reduce the CPU time and to increase the reliability of the results.

We can see the difference of the two methods by plotting the local density profile of molecules in a slitpore. We use the local density function $\zeta_i(Z)$ defined by equation (10) for representing the local density profile [19].

$$\zeta_i(Z) = \rho_i(Z)/x_i\rho_p \tag{10}$$

If the local density profile is uniform in the pore, $\zeta_i(Z)$ becomes unity in the whole region. The curves of $\zeta_i(Z)$ for each component should be symmetric if a simulation run is done well to attain equilibrium. Figure 3 shows the local density function $\zeta_i(Z)$ to compare the performance of the conventional μVT and the modified μVT method calculated at $T = 313.2$ K and $p^* = 0.272$ for $H = 1.2$ nm and $k_{2s} = 0.0$. At this point,

Table 2 Comparison of performance between conventional μVT(1) and μVT with particle exchange (2); T= 313.2 K, H = 1.2 nm, $y_2 = 0.001$.

	ρ_f^*	p^*	ρ_p^*	x_1	U_p^*	$f_{success}$
(1)	0.001	0.00139 (-)	0.188 (2)	0.134 (4)	−24.48 (7)	3×10^{-4}
(2)			0.191 (2)	0.126 (6)	−24.75 (12)	1×10^{-2}
(1)	0.005	0.00685 (1)	0.237 (2)	0.298 (6)	−22.04 (22)	4×10^{-5}
(2)			0.235 (4)	0.277 (11)	−22.46 (22)	8×10^{-3}
(1)	0.010	0.0135 (-)	0.262 (1)	0.375 (5)	−20.81 (9)	3×10^{-5}
(2)			0.264 (4)	0.372 (11)	−20.92 (21)	6×10^{-3}
(1)	0.050	0.0598 (2)	0.327 (4)	0.551 (27)	−17.89 (55)	1×10^{-5}
(2)			0.323 (5)	0.525 (11)	−18.41 (18)	5×10^{-3}
(1)	0.100	0.102 (1)	0.353 (8)	0.623 (48)	−16.59 (95)	5×10^{-6}
(2)			0.346 (3)	0.594 (8)	−17.15 (16)	6×10^{-3}
(1)	0.300	0.165 (8)	0.390 (11)	0.735 (32)	−14.45 (61)	1×10^{-5}
(2)			0.387 (6)	0.717 (13)	−14.82 (27)	1×10^{-2}
(1)	0.500	0.272 (26)	0.422 (6)	0.823 (13)	−12.73 (24)	1×10^{-5}
(2)			0.414 (2)	0.799 (6)	−13.20 (1)	7×10^{-3}

The numbers in parentheses are the standard deviations in units of the last decimal digit of the corresponding quantity. The symbol (-) indicates that the standard deviation is smaller than the last digit.

2.1×10^8 trials result in about 5000 successes for creation or destruction of benzene in the conventional μVT method, while 1.5×10^7 trials result in about 30000 successes for exchange by use of the modified μVT method. Both curves for CO_2 and benzene are not symmetric in Figure 3 (a), which indicates a lack of sufficient sample points in the conventional μVT ensemble. On the other hand they are symmetric in Figure 3 (b) by use of the μVT ensemble with particle exchange. We may conclude that the modified μVT ensemble method with particle exchange can make the simulation system reach the equilibrated state quickly and yield reliable results.

4.3 Effect of Temperature

Figure 4 shows the chemical potentials of CO_2 and benzene at two temperatures, 313.2 K and 323.2 K, for a fluid mixture of mole fraction $y_2 = 0.001$. The ordinate is the dimensionless chemical potential, $\mu_i^* = \mu_i/kT$, and the abscissa is the dimensionless pressure. At both temperatures, the chemical potential curves for CO_2 increase monotonically with increasing pressure, while the curves for benzene have a maximum at nearly $\rho^* = 0.06$ and then they decrease. We may refer to this decrease as the enhanced solubility in a supercritical fluid. At T= 323.2 K, the chemical potential curve for benzene is slightly higher in the SCF region than the curve at T= 313.2 K, which we may call the "density effect" on the chemical potential since in the SCF region the decrease in density at higher temperatures results in the decrease in the attractive interactions between a solute molecule and solvent molecules. Figure 5 shows the true adsorptions of benzene and CO_2 at 313.2 K and 323.2 K for $H = 2$ nm and $k_{2s} = 0.0$. The ordinate is the dimensionless true adsorption, $\sigma_{ii}^2 \Gamma_{t,i}$, which is defined in equation (11) as the number of molecules of component i per unit surface area.

$$\Gamma_{t,i} = \langle N_{i,p} \rangle / 2A = \rho_p x_i H/2 \tag{11}$$

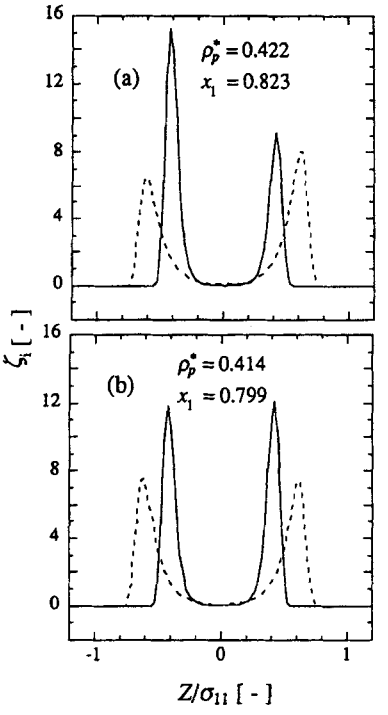

Figure 3 The local density function $\zeta_i(Z)$ of CO_2 and benzene in a pore: (a) conventional μVT (b) modified μVT with particle exchange; $H = 1.2$ nm, $T = 313.2$ K, $y_2 = 0.001$, $p^* = 0.272$; the soild line is benzene and the dotted line is CO_2.

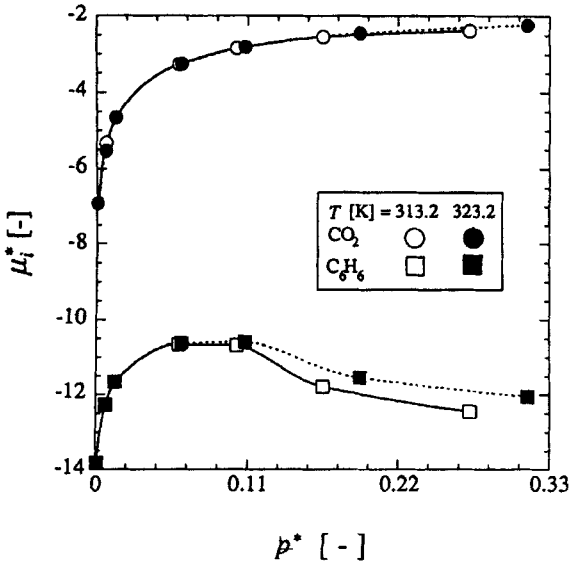

Figure 4 The chemical potentials of CO_2 and benzene, μ_i^*, for a binary mixture of $y_2 = 0.001$ at 313.2 K and 323.2 K.

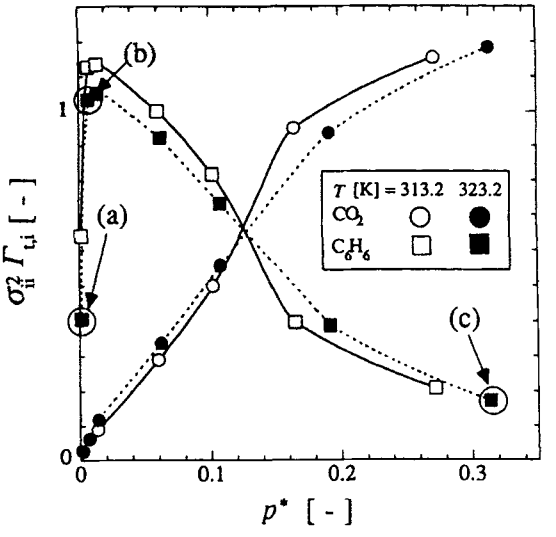

Figure 5 The true adsorptions of C_6H_6 and CO_2 from a mixture of $y_2 = 0.001$ into a pore of slitwidth $H = 2$ nm at 313.2 K and 323.2 K.

The curves for benzene show a maximum ($p^* = 0.007$) at a pressure far below the critical pressure of CO_2 ($p_c^* = 0.142$) and decrease with an increase in pressure. On the other hand, the adsorption of CO_2 increases monotonically with increasing pressure. There are two important observations. One is that the pressure corresponding to the maximum point for the chemical potential of benzene is not the same pressure for the adsorption maximum; the latter is much lower. Therefore, we can conclude that the competitive character of adsorption between benzene and CO_2 plays an important role in this case. The increase in the chemical potential of CO_2 accelerates the adsorption of CO_2, which results in the desorption of benzene due to the competitive adsorption. Another observation is that the amount of benzene adsorbed decreases with increasing temperature in the low pressure region. On the other hand, in the SCF region it increases with increasing temperature as shown in the figure. This inverse is attributable to the so called the "density effect" for the chemical potential in SCF.

Figure 6 shows the local density function, $\zeta_i(Z)$ at point (a), (b) and (c) in Figure 5 at 323.2 K. In the low pressure region, benzene molecules occupy the first monolayer near the wall (Fig. 6 (a)), and the curve of CO_2 swells in the middle region of the pore (Fig. 6 (b)). The change of the CO_2 – curve – shape is understandable because CO_2 molecules have to find their position in the middle region of the pore. At a higher pressure, however, CO_2 curve resembles that of pure CO_2 because the pore is again filled almost by CO_2 molecules (Fig. 6 (c)).

4.4 *Effect of Binary Parameter* k_{2s}

Figure 7 represents the influence of the binary parameter k_{2s} on the true adsorption of a solute (2) at $T = 313.2$ K for $H = 2$ nm slitpore to show the effect of interactions

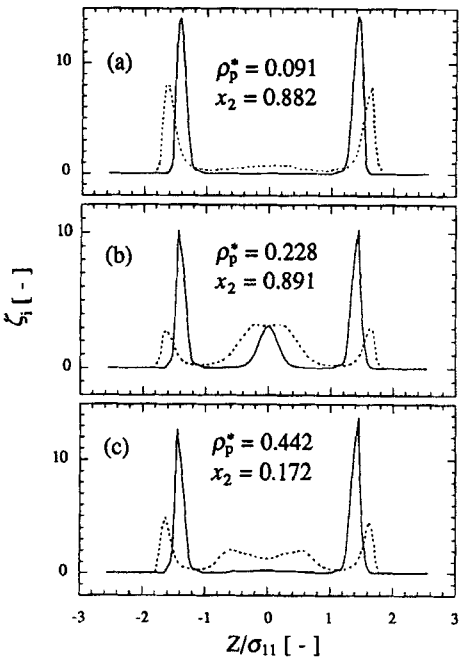

Figure 6 The local density function $\zeta_i(Z)$ for CO_2 (1) + benzene (2) mixtures in a pore of width $H = 2$ nm at $T = 323.2$ K; the soild line is benzene and the dotted line is CO_2

between solute molecules and surface carbon. The amount of adsorption of a solute diluted in CO_2 increases with an increase in the solute – surface interaction (decrease in k_{2s}). We may expect from this result that there might be a case that the desorption by SCF is not effective for a substance strongly adsorbed in a pore. The potential depth for interactions between adsorbate and surface carbon is the most sensitive factor for the adsorption from the supercritical fluid since the adsorption equilibrium is essentially determined by the Boltzmann factor, $\exp(-\Phi_i/kT)$. Figure 8 shows the local density function $\zeta_i(Z)$ of CO_2 and benzene at point (a) ($k_{2s} = -0.15$) and (b) ($k_{2s} = 0.0$) in Figure 7. It is shown that CO_2 molecules are forced to be in the middle of the pore for $k_{2s} = -0.15$ much more than those for $k_{2s} = 0.0$.

4.5 *Effect of Slitwidth*

Figure 9 shows the external potentials of single molecules, CO_2 and benzene, in two pores of width $H = 2$ nm and 1.2 nm. The potential curves for CO_2 and benzene become deeper in a narrower pore since a molecule feels deeper attractive potential from an adjacent wall so far the slitwidth is large enough to accommodate at least one molecule. We also note that in the narrower pore the potential curve of benzene becomes much deeper than that of CO_2; therefore, the effect of narrowing slitwidth

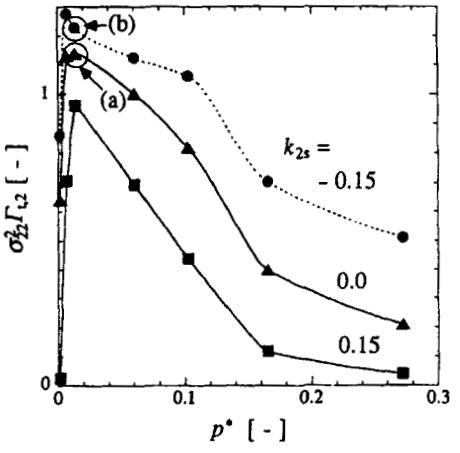

Figure 7 Effect to k_{2s} on the true adsorption of C_6H_6 from a mixture of $y_2 = 0.001$ into a pore of slitwidth $H = 2$ nm at 313.2 K.

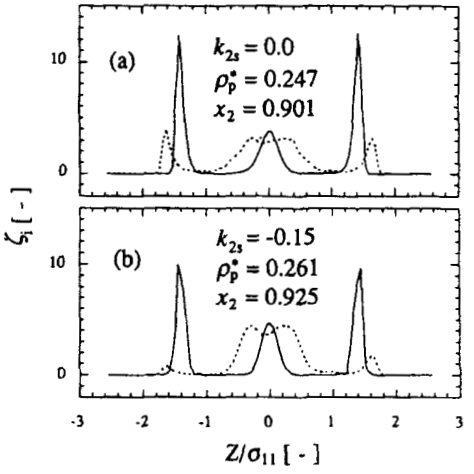

Figure 8 The local density function $\zeta_i(Z)$ for CO_2 + benzene mixtures in a pore of slitwidth $H = 2$ nm at $T = 313.2$ K: (a) and (b) correspond to states (a) and (b) in Figure 7, respectively; the soild line is benzene and the dotted line is CO_2.

resembles increasing the benzene-surface interaction (decreasing a parameter k_{2s}). Figure 10 shows the influence of the slitwidth on the true adsorptions of CO_2 and benzene. The adsorption capacity per unit surface area decreases with a decrease in the slitwidth and the isotherm curve for benzene in the narrower pore decreases gradually with increasing pressure in the high pressure region. The gradual decrease of the benzene curve is attributed to the relative increase in the benzene-surface interaction as mentioned above.

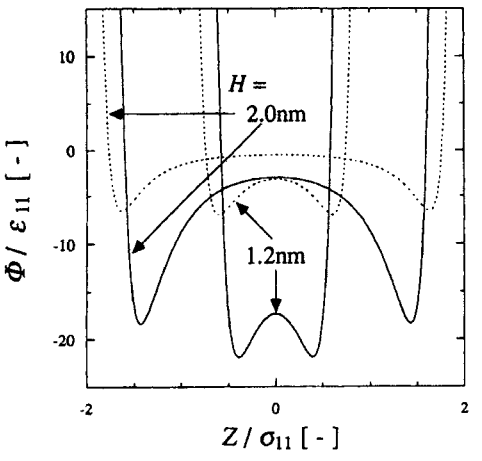

Figure 9 Potentials of single molecules vs. distance normal to the wall surface in pores of slitwidth $H = 2\,\text{nm}$ and 1.2 nm at $T = 313.2$ K for $k_{2s} = 0.0$; the soild line is benzene and the dotted line is CO_2.

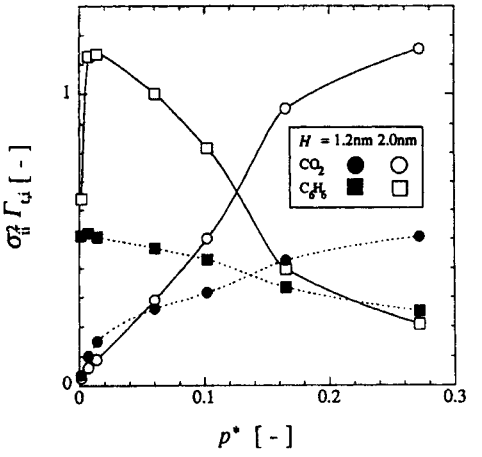

Figure 10 Effect of slitwidth on the true adsorption of CO_2 (1) and benzene (2) from a mixture of $y_2 = 0.001$ at 313.2 K: the number in the figure denote slitwidth in nm.

5 CONCLUSIONS

The NVT and μVT ensemble MC methods have been used for computing binary adsorptions in a slitpore in equilibrium with dilute benzene in supercritical CO_2. The particle exchange trials in the μVT ensemble have improved the probability of acceptance for creation and destruction of larger molecules. The LJ potential function has been used for representing intermolecular interactions between CO_2, benzene and surface graphitic carbon. Adsorptions of benzene from supercritical CO_2

show a maximum at $p \ll p_c$, CO_2 and then decrease with increasing pressure, while adsorptions of CO_2 increase monotonically with increasing pressure. It has been shown that the enhanced solubility in supercritical CO_2 is the major reason for the decrease in benzene adsorption; the competitive adsorption of CO_2 is the second reason. The cross of the true adsorption curves caused by the "density effect" has been demonstrated by varying temperature 313.2 K to 323.2 K. When the interaction potential of a solute molecule exerted from two surfaces becomes deep, the adsorption isotherm increases to overcome the enhanced solubility and the competitive adsorption of the SCF. There might be a case that the SCF does not work for regeneration of spent adsorbents contaminated by large molecules.

Acknowledgements

This research was supported by a Grant-in-Aid for Scientific Research on Priority Areas No. 04238105 from the Ministry of Education, Japan.

References

[1] M. A. McHugh and V. J. Krukonis, *Supercritical Fluid Extraction, Principles and Practice*, 2nd ed., Butterworths. (1994)
[2] T. J. Bruno and J. F. Ely, *Supercritical Fluid Technology: Reviews in Modern Theory and Applications*, CRC Press (1991)
[3] M. Saito, Y. Yamauchi and T. Okuyama, (eds), *Fractionation by Packed-Column SFC and SFE: Principles and Applications*, VCH, New York. (1994)
[4] M. D. L. de Castro, M. Valcarcel and M. T. Tena, *Analytical Supercritical Fluid Extraction*, Springer-Verlag, Berlin (1994)
[5] S. Takishima, H. Matsumoto, H. Nagasaki, H. Masuoka, Y. Mukai and T. Sakai: "Debindering from alumina green body by combined use of the supercritical fluid extraction technique and active carbon", *Kagaku Kogaku Ronbunshu*, **17**, 716–724 (1991).
[6] G. Madras, C. Erkey and A. Akgerman, "Supercritical fluid regeneration of activated carbon loaded with heavy molecular weight organics", *Ind. Eng. Chem. Res.*, **32**, 1163–1168 (1993).
[7] H. Uchida, T. Matsuki, T. Furuya, Y. Iwai and Y. Arai, "Effects of pressure and temperature on adsorptive separation of isomers of dimethylnaphthalene dissolved in supercritical carbon dioxide", Proc. of the 59th Annual meeting of the *Soc. of Chem. Engs.*, Japan, L304, Sendai (1994).
[8] W. van Megen, and I. K. Snook, "Physical adsorption of gases at high pressure, III. Adsorption in slit-like pores", *Mol. Phys.*, **54**, 741–755 (1985).
[9] K. R. Matranga, A. L. Myers and E. D. Glandt, "Storage of natural gas by adsorption on activated carbon", *Chem. Eng. Sci.*, **47**, 1569–1579 (1992).
[10] M. J. Bojan, R. van Slooten, and W. Steele, "Computer simulation studies of the storage of methane in microporous carbons", *Separation Science and Technology*, **27**, 1837–1856 (1992).
[11] T. Nitta, M. Nozawa and Y. Hishikawa, "Monte Carlo Simulation of adsorption of Gases in Carbonaceous Slitlike Pores", *J. Chem. Eng. Japan*, **26**, 266–272 (1993).
[12] S. Sokolowski, and J. Fisher, "Lennard-Jones mixtures in slit-like pores: a comparison of simulation and density-functional theory", *Molec. Phys.*,**71**, 393–412 (1990).
[13] T. F. Meister, and D. M. Kroll, "Density-functional theory for inhomogeneous fluids: Application to wetting", *Phys. Rev.*, **A31**, 4055–4057 (1985).
[14] R. D. Groot, "Density functional models for inhomogeneous hard sphere fluids", *Molec. Phys.*, **60** 45–63 (1987).
[15] R. F. Cracknell, D. Nicholson and N. Quirke, "A grand canonical Monte Carlo study of Lennard-Jones mixtures in slit shaped pores", *Mol Phys.*, **80**, 885–897 (1993).
[16] Z. Tan, and K.E. Gubbins, "Selective adsorption of simple mixtures in slit pores: A model of methane-ethane mixtures in carbon", *J. Phys. Chem.*, **96**, 845–854 (1992).
[17] E. Kierlik, M. Rosenberg, J. E. Finn and P. A. Monson, "Binary vapour mixtures adsorbed on a graphite surface: A comparison of mean field density functional theory with results from Monte Carlo simulations", *Molec. Phys.*, **75**, 1435–1454 (1992).

[18] T. Okayama, J. Yoneya and T. Nitta, "Monte Carlo Simulations of Adsorption in a Slitlike Pore for Binary Mixtures of Butane and Carbon Dioxide at Supercritical Conditions", *Fluid Phase Equilibria* (in Press).
[19] T. Nitta, and J. Yoneya, "Computer Simulations for Adsorption of Benzene Diluted in Supercritical Carbon Dioxide", *J. Chem. Eng. Japan*, **28**, 31–37 (1995).
[20] J. J. Nicolas, K. E. Gubbins, W. B. Streett and D. J. Tildesley: "Equation of state for the Lennard-Jones fluid" , *Mol. Phy.*, **37**, 1429–1454(1979)
[21] W. A.: Steele, *Surface Sci.*, **36**, 317–352 (1973); *The Interaction of Gases with Solid Surfaces*, Pergamon Press, Oxford (1974).
[22] M. K. Gupta, Y.-H. Li, B. J. Hulsey and R. L. Robinson, Jr.: "Phase equilibrium for carbon dioxide-benzene at 313.2, 353.2, and 393.2 K", *J. Chem. Eng. Data*, **27**, 55–57 (1982)
[23] T. Nitta, M. Nozawa and S. Kida, "Gas-Phase Adsorption Characteristics of High-Surface Area carbons Activated from Meso-Carbon Micro-Beads", *J. Chem. Eng. Japan*, **25**, 176–182 (1992)
[24] A. Z. Panagiotopoulos, "Direct determination of phase coexistence properties of fluids by simulation in a new ensemble", *Mol. Phys.*, **61**, 813 (1987); *ibid.*, **62**, 701–719 (1987)
[25] M. P. Allen, and D. J. Tildesley, *Computer Simulation of Liquids*, Clarendon Press, Oxford, (1987).